E. Perilli, M. Cantley, V. Marino, T. N. Crotti, M. D. Smith, D. R. Haynes and A. A. S. S. K. Dharmapatni

Quantifying not only bone loss, but also soft tissue swelling, in a murine inflammatory arthritis model using micro-computed tomography

Scandinavian Journal of Immunology, 2015; 81(2):142-150

Originally published at:
http://doi.org/10.1111/sji.12259

doi: 10.1111/sji.12259

Quantifying Not Only Bone Loss, but Also Soft Tissue Swelling, in a Murine Inflammatory Arthritis Model Using Micro-Computed Tomography

E. Perilli*, M. Cantley†, V. Marino‡, T. N. Crotti†, M. D. Smith§¶, D. R. Haynes† & A. A. S. S. K. Dharmapatni†

*Medical Device Research Institute, School of Computer Science, Engineering & Mathematics, Flinders University, Bedford Park, SA, Australia; †Discipline of Anatomy and Pathology, School of Medical Sciences, The University of Adelaide, Adelaide, SA, Australia; ‡School of Dentistry, The University of Adelaide, Adelaide, SA, Australia; §Department of Rheumatology, Flinders Medical Centre and Flinders University, Bedford Park, SA, Australia; and ¶Rheumatology Research Unit, Repatriation Hospital, Daw Park, SA, Australia

Received 1 July 2014; Accepted in revised form 12 November 2014

Correspondence to: E. Perilli, Medical Device Research Institute, School of Computer Science, Engineering and Mathematics, Flinders University, GPO Box 2100, Adelaide, SA 5001, Australia.
E-mail: egon.perilli@flinders.edu.au

Abstract

In rodent models of inflammatory arthritis, bone erosion has been non-invasively assessed by micro-computed tomography (micro-CT). However, non-invasive assessments of paw swelling (oedema) are still based on clinical grading by visual evaluation, or measurements by callipers, not always reliable for the tiny mouse paws. The aim of this work was to demonstrate a novel straightforward 3D micro-CT analysis protocol capable of quantifying not only joint bone erosion, but also soft tissue swelling, from the same scans, in a rodent inflammatory arthritis model. Balb/c mice were divided into two groups: collagen antibody-induced arthritis (CAIA) and CAIA treated with prednisolone, the latter reflecting an established treatment in human rheumatoid arthritis. Clinical paw scores were recorded. On day 10, front paws were assessed by micro-CT and histology. Micro-CT measurements included paw volume (bone and soft tissue together) and bone volume at the radiocarpal joint, and bone volume from the radiocarpal to the metacarpophalangeal joint. Micro-CT analysis revealed significantly lower paw volume (-36%, $P < 0.01$) and higher bone volume ($+17\%$, $P < 0.05$) in prednisolone-treated CAIA mice compared with untreated CAIA mice. Paw volume and bone volume assessed by micro-CT correlated significantly with clinical and histological scores ($|r| > 0.5$, $P < 0.01$). Untreated CAIA mice showed significantly higher clinical scores, higher inflammation levels histologically, cartilage and bone degradation, and pannus formation, compared with treated mice ($P < 0.01$). The presented novel micro-CT analysis protocol enables 3D-quantification of paw swelling at the micrometre level, along with the typically assessed bone erosion, using the same images/scans, without altering the scanning procedure or using contrast agents.

Introduction

Rheumatoid arthritis (RA) is an autoimmune, chronic, destructive inflammatory disease that predominantly affects the synovial joints. Within the affected joints, there is a steady progression of synovial hyperplasia and neovascularization, mixed mononuclear and granulocytic cellular infiltration, damage to articular cartilage, bone remodelling, proliferation and phenotypic changes of synovial fibroblasts [1, 2]. Clinically, this manifests as joint swelling, erythema and pain, which can progress to bone erosion with obvious joint architecture changes and disability [3].

Due to the complexity of RA, various animal models are necessary to increase our understanding of the disease aetiology and to investigate the effects of new drugs on disease initiation and progression. The collagen antibody-induced arthritis (CAIA) mouse model has similar features to human RA that provides a straightforward and rapid means of producing this pathology, bypassing the requirement for cognate immune response [4–8]. Hence, it is an appropriate model to investigate the effector phase of the disease such as synovitis and bone erosion within the joint.

Recent studies, including those in our own laboratory, have utilized micro-computed tomography (micro-CT) to quantify bone erosion in murine models of inflammatory arthritis [9, 10]. Micro-CT allows for the non-destructive quantification and visualization of bone changes at the micrometre level in 3D in *in vitro* and *in vivo* studies. It has been extensively used in osteoporosis and osteoarthritis

SCANDINAVIAN JOURNAL OF Immunology AN INTERNATIONAL MONTHLY JOURNAL

studies [11–16] as well as RA [9, 10, 17–19]. However, in RA studies, the typical non-invasive read-outs of the disease severity in terms of *oedema* (erythema and swelling) are commonly based on clinical grading, which are the measurements based on a subjective visual evaluation by an operator [6, 9, 17, 18, 20–22]. Quantitative methods to assess swelling include measuring paw thickness using a calliper [3] or a plethysmometer [10]. Both these methods, however, might not always be practical and are relatively difficult particularly due to the small paw size in mice [23].

Studies utilizing micro-CT analysis in rodent models of RA have focussed on high-resolution quantification of bone erosion. However, precise measurement of oedema (swelling) in these models still remains limited and is still commonly assessed using other methods as described above. Hence, the question arises as to whether the readily available micro-CT images can also be used for quantifying the paw swelling in terms of paw volume, at the micrometre level in 3D [9, 10, 18]. Indeed, in soft tissue studies on mice, micro-CT has been used to visualize and quantify soft tissue such as lungs or body fat, in 3D [24–28]. Hence, micro-CT could also be used to measure soft tissue swelling, in rodent models of RA.

Prednisolone is an established RA treatment in humans which suppresses inflammation and prevents bone damage in a CAIA mouse model [3, 29]. A comparison of CAIA mice and prednisolone-treated CAIA mice was therefore used in this study, as it is likely that marked differences in both joint inflammation and bone erosion would be noted between the two mouse groups [3, 29].

The aim of this study was to demonstrate a novel 3D micro-CT image analysis protocol capable of visualizing and quantifying both paw swelling and joint bone erosions within the same micro-CT scans, in a murine inflammatory arthritis model. Results were compared with a previously established clinical paw score method and histological assessments [7, 9].

The hypothesis was that there would be a significantly higher paw volume (paw swelling) and lower bone volume (bone resorption) as detected by micro-CT in CAIA mice compared with prednisolone-treated CAIA mice, and that these changes would correlate with changes in clinical paw scores and histological scores.

Materials and methods

Animals and collagen antibody induced arthritis induction. All experiments were performed in accordance with the NHMRC Australian Code of practice for the care and use of animals for scientific purposes, with approval from the Animal Ethics Committees of both the University of Adelaide and SA Pathology (Approval Nos M-2009-167 and 75/09, respectively). Female Balb/c mice (6–8 weeks old) were divided into two groups: group 1 (CAIA group, $n = 10$) and group 2 (CAIA treated with prednisolone group, $n = 12$). Arthritis was induced using the CAIA protocol as previously published [9]. Briefly, on day 0, all mice were injected with a 150 μl (1.5 mg) cocktail of monoclonal antibody to collagen type 2 (Chondrex Inc., Redwood, WA, USA) via tail vein. On day 3, mice were injected with 20 μl (10 μg) *E. Coli* LPS intraperitoneally. Prednisolone treatment (10 mg/kg/day) was given to mice in group 2 via oral gavage for 7 days, commencing on day 4 and continued daily until the study completion at day 10. CAIA mice were given vehicle (PBS/10%; EtOH) only.

Clinical paw scoring. Clinical paw scores were recorded daily from day 0 to 10 by two independent observers that were blinded as to the group allocation; groups were randomly presented to them for scoring, based on the previously published methods (total score per paw: 0 = normal, 15 = severe) [7]. Each paw was scored according to the severity of inflammation in the wrist (radiocarpal joint) or ankle/metatarsal and the involvement of the small joints. Briefly, the score ranged between 0 and 5 for severity of wrist/ankle swelling, and was 1 for each digital joint involved; hence, a maximal score of 15 for each paw and the maximal score for each mouse could be 60. Daily clinical observations of general health including body weight were recorded on clinical record sheets. After 10 days, mice were humanely killed using CO_2 inhalation, and front paws were collected for micro-CT and histological analysis. Based on the clinical scoring, 90% of the CAIA mice demonstrated the highest scores in the front right paws; therefore, the front right paws were selected for analysis.

Micro-CT analysis. After collection, the front right paws were fixed in 10% buffered formalin overnight followed by washing in phosphate-buffered saline and then wrapped in cling wrap for micro-CT scanning the following day (micro-CT SkyScan model 1076; SkyScan-Bruker, Kontich, Belgium). During scanning, the paws were placed in the scanner with the long axis aligned with the axis of the scanner bed. The scanning parameters were as follows: pixel size 17.4 μm, tube voltage 74 kV, tube current 136 μA, aluminium filter 1.0 mm, rotation step 0.5°, frame averaging of 1 and scanning time 12 min [9]. The cross-section images were then reconstructed using a filtered back-projection algorithm (NRECON software, V 1.12.04; SkyScan) and saved as 8-bit grey-level files (bitmap format). For each paw, a stack of up to 475 cross sections was reconstructed, with an interslice distance of 1 pixel (17.4 μm), corresponding to a maximum reconstructed height of 8.3 mm (Fig. 1), recreating the full length of the paw. For all animals, the reconstructed cross-section images were realigned in 3D, with the long axis of the paw aligned along the vertical (inferior–superior) direction of the images (software DATAVIEWER, SkyScan) (Fig. 1).

Volume of interest selection. The volume scanned and reconstructed by micro-CT comprised the entire paw (Fig. 1). From the stack of contiguous cross-section images, two cylindrical volumes of interest (VOIs) of

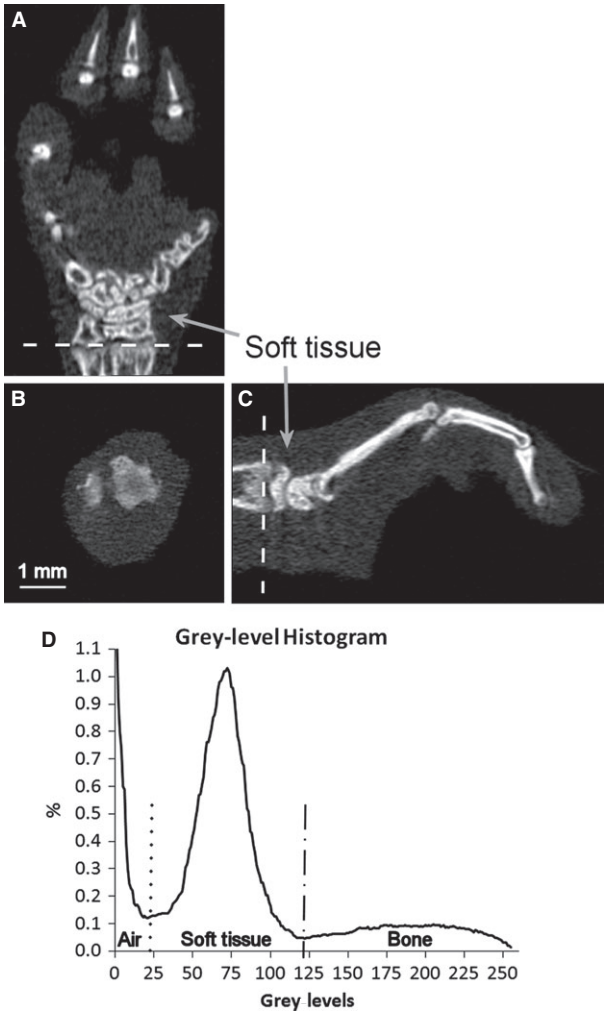

Figure 1 Cross-sectional micro-CT images of a front paw, in coronal (A), transaxial (B) and sagittal view (C). The grey-scale images show the bone (in bright grey), surrounded by the soft tissue (in dark grey, indicated by arrows). A cross section of the epiphyseal growth plate is shown (B), with its position indicated by dashed line (A, C), used as landmark for selection of the lengths of the volumes of interest for quantitative micro-CT analysis (Fig. 2). A grey-level histogram (256 grey levels) is shown (D), with the minimum threshold level used for segmentation of the paw (soft tissue and bone together) indicated by a dotted line (value = 22), and the minimum threshold level for the bone only, indicated by a dash-dotted line (value = 120), respectively.

different length were selected by taking the position of the epiphyseal growth plate (EGP) as a reference (Fig. 1) (software CT ANALYSER, V.1.12.0; SkyScan). The diameter of the VOIs was standardized to 4.5 mm for all animals, so that it was large enough to enclose the whole paw including soft tissue. The selection of the two VOIs (software CT ANALYSER) was made as follows: (1) 'Radiocarpal joint-to-metacarpophalangeal (MCP) joint VOI': the VOI extended 40 slices proximally from the EGP and extended distally through the whole metacarpus to the MCP joint including each proximal phalanx for 35 slices, corresponding to a maximum length (midfinger) of 325 slices from the EGP (i.e. 5.65 mm), that is a total maximum length of the VOI of 365 slices (i.e. 6.35 mm, Fig. 2B); (2) 'Radiocarpal joint VOI': the VOI extended 40 slices proximally and 100 slices distally from the EGP (total VOI length = 140 slices, i.e. 2.44 mm, standardized on all the mice, Fig. 2C, D and E).

Image thresholding, calculation of paw volume and bone volume. In the grey-level histogram of the reconstructed cross-section images (bitmap format, 256 grey levels, ranging from 0 to 255), the grey-level values in the lower range (from 0 to 21) corresponded to air or background, followed in increasing order by values of the soft tissue (ranging from 22 to 119) and bone (from 120 to 255) (Fig. 1D). Two fixed minimum threshold values were applied to all the specimens for segmentation; one for segmenting the paw (soft tissue and bone together, by setting the minimum threshold level to 22, the maximum to 255) and leaving air as background, and a second minimum threshold level for segmenting the bone pixels only (from minimum 120 to maximum 255), leaving air and soft tissue as background [14, 27, 30] (Fig. 1D). By applying the corresponding threshold values, automated calculations were performed of paw volume (PV, expressed in mm^3) and bone volume (BV, expressed in mm^3) (software CT ANALYSER). The PV was measured over the radiocarpal joint VOI (Fig. 2E). The BV was measured both over the radiocarpal joint VOI (Fig. 2C) and the radiocarpal-to-MCP joint VOI (Fig. 2B). The PV was calculated as the volume occupied by the voxels segmented as 'paw', that is bone and soft tissue; the BV was calculated as the volume occupied by the voxels segmented as 'bone'. After segmenting the paw, loose speckles in the segmented images which originated from noise pixels having their grey-level values close to those of soft tissue were removed, using a cycle of the software function 'sweep' (software CT ANALYSER) [31]. This automatically removes all but the largest object in the 3D volume, maintaining the paw as the largest object. All the volumes were quantified using the marching cubes method (software CT ANALYSER) [11, 14, 32, 33].

Histological analysis. After micro-CT scanning, the paws were decalcified in 10% EDTA solution for 10 weeks and processed for paraffin embedding and sectioning (5 μm thick), for histological analysis (haematoxylin and eosin staining), according to previously published methods [9]. Histological analysis comprised scores for inflammation, pannus formation, cartilage and bone degradation [9]. Sections were then analysed by two independent, blinded observers.

Inflammation scoring (score 0–3) was performed on the soft tissue within the radiocarpal joint, based on the number of inflammatory cells (lymphocytes, plasma cells, neutrophils or macrophages), as follows: normal tissue (<5% inflammatory cells) was scored 0, mild inflammation (5–20% inflammatory cells) = 1, moderate

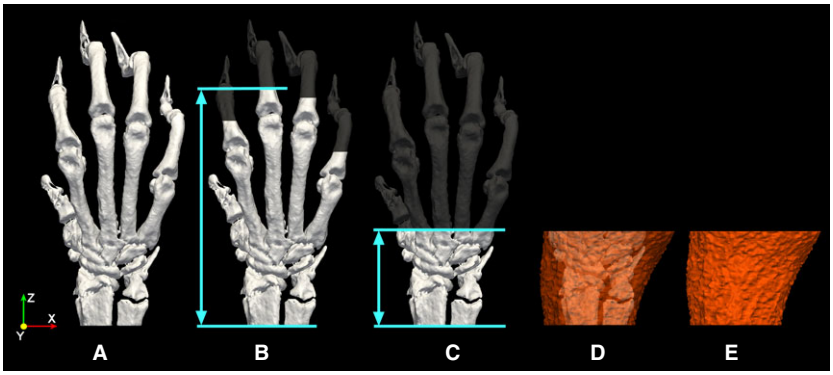

Figure 2 3D micro-CT images of a front right paw with bone segmented in white colour (A–C) and soft tissue in red colour (E). In (D), the bone is visible with the soft tissue in transparency. The lengths of the volumes of interest (VOIs) used for micro-CT analysis (vertical arrows): radiocarpal-to-metacarpophalangeal joint VOI (B) (maximum length 6.35 mm); radiocarpal joint VOI (C–E) (standard length 2.44 mm for all the mice).

inflammation (21–50% inflammatory cells) = 2 and severe inflammation with a massive immune cell infiltration (>50% of cells) = 3 [9].

Cartilage and bone degradation score (0–3): score 0 = normal bone integrity, score 1 = mild cartilage destruction, score 2 = evidence of both cartilage and bone destruction and score 3 = severe cartilage and bone destruction.

Pannus formation (synovial membrane with infiltration of inflammatory cells): score 0 = no pannus formation; score 1 = pannus formed [9].

Statistical analysis. Differences between groups in clinical paw scores, histological scores, PV and BV were assessed using Mann–Whitney *U*-test. Correlations between these parameters were analysed using the Pearson's product-moment correlation. The significance level was set to $P < 0.05$. All statistical analyses were performed using SPSS version 20 (Chicago, IL, USA).

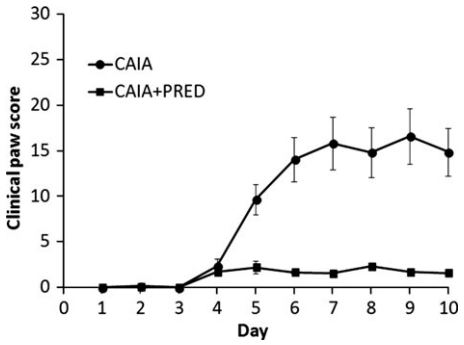

Figure 3 Daily clinical paw scores, average values and standard error of the mean (error bars) for each group [$n = 10$ animals for the CAIA group, $n = 12$ animals for the prednisolone-treated group (CAIA + PRED)]. The disease incidence was 90% in the CAIA group, with 90% of the mice showing a clinical score ≥5 by day 7, until the end of the study. As the highest scores were in the front right paw (90% of the animals), the front right paw was chosen for comparisons with micro-CT analysis and histology.

Results

The disease incidence was 90% in the CAIA group, with nine mice out of 10 showing a clinical score ≥5 by day 7, until the end of the study, as opposed to the prednisolone-treated CAIA group (treatment started at day 4), which showed abrogation of the disease for the entire duration of the experiment (Fig. 3). All the examined front right paws were successfully analysed by micro-CT and histology. Table 1 summarizes the average values, standard deviations, and minimum and maximum values for the parameters and scores examined.

Micro-CT analysis of paw swelling and bone erosion

Micro-CT analysis revealed a significantly lower PV in prednisolone-treated CAIA mice compared with the untreated CAIA mice (−36%, $P < 0.001$) (Table 1, Fig. 4). The BV was significantly higher within the radiocarpal joint (+17%, $P < 0.05$) and within the radiocarpal-to-MCP joint (+14%, $P < 0.05$) in prednisolone-treated CAIA mice than in CAIA mice (Table 1, Fig. 4).

In Fig. 5, 3D micro-CT images of the front paws are presented, with the CAIA mouse exhibiting bone erosion (Fig. 5a) and paw swelling (Fig. 5C,E), compared with the prednisolone-treated CAIA mouse (Fig. 5B,D and F, respectively).

Histological and clinical score analysis

Consistent with the micro-CT results, histological assessments revealed significantly higher levels of inflammation (2.40 ± 1.26 versus 0.00 ± 0.00, $P < 0.01$), of cartilage and bone degradation (2.00 ± 1.15 versus 0.00 ± 0.00, $P < 0.01$), of pannus formation (0.07 ± 0.38 versus 0.00 ± 0.00, $P < 0.01$), and clinical paw scores (6.10 ± 3.69 versus 0.71 ± 0.45, $P < 0.001$) in CAIA mice compared with those in prednisolone-treated CAIA mice (Table 1, Fig. 6).

Correlations: micro-CT measurements (PV and BV) versus histological and clinical scores

The paw volume and bone volume assessed by micro-CT correlated significantly with histological and clinical scores (Table 2). The PV was strongly and directly related to the

Table 1 Summary (front right paws): paw volume and bone volume assessed by micro-CT, histological and clinical scores.

	$n = 10$		$n = 12$		
	CAIA		CAIA + PRED		
	Avg ± SD	Min, max	Avg ± SD	Min, max	*P*-value
Micro-CT					
PV_{RC} (mm^3)	24.0 ± 5.7	16.3, 30.9	15.5 ± 1.5	13.0, 17.7	<0.001
BV_{RC} (mm^3)	1.37 ± 0.21	0.98, 1.55	1.60 ± 0.16	1.31, 1.77	0.012
$BV_{RC\text{-}MCP}$ (mm^3)	2.63 ± 0.39	1.97, 3.04	3.00 ± 0.22	2.63, 3.35	0.025
Histological scores					
Inflammation (0–3)	2.40 ± 1.26	0, 3	0.00 ± 0.00	0, 0	<0.01
Cartilage and bone degradation (0–3)	2.00 ± 1.15	0, 3	0.00 ± 0.00	0, 0	<0.01
Pannus formation (0–1)	0.70 ± 0.48	0, 1	0.00 ± 0.00	0, 0	<0.01
Clinical score (0–15)	6.10 ± 3.69	1, 12	0.71 ± 0.45	0, 1	<0.001

PV_{RC}, paw volume in radiocarpal joint; BV_{RC}, bone volume in radiocarpal joint; $BV_{RC\text{-}MCP}$, bone volume in radiocarpal-to-metacarpophalangeal joint. Values reported in table as average±standard deviation, minimum and maximum values.
P-value: *P*-value (Mann–Whitney test) for the comparison between the CAIA mice and the CAIA mice treated with prednisolone (CAIA + PRED).

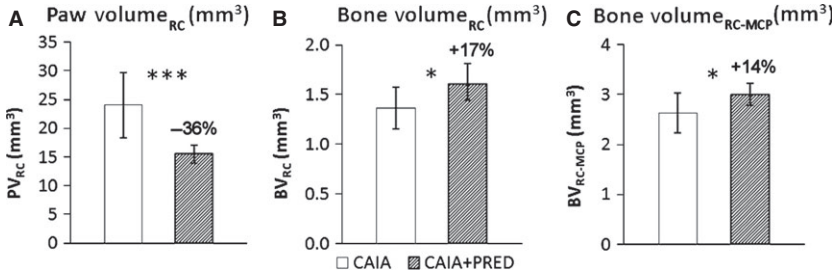

Figure 4 Bar graphs, reporting average value and standard deviation (error bars) of the 3D measurements made by micro-CT: paw volume in radiocarpal joint (A), bone volume in radiocarpal joint (B) and bone volume in radiocarpal-to-metacarpophalangeal (MCP) joint (C). The indicated percentage value is the percentage difference in average value between CAIA group and prednisolone-treated CAIA group (CAIA+PRED). *: $P < 0.05$, ***: $P < 0.001$ (Mann–Whitney).

cartilage and bone degradation score ($r = 0.912$, $P < 0.0001$), inflammation score ($r = 0.855$, $P < 0.0001$) and clinical score ($r = 0.868$, $P < 0.0001$). The BV was inversely correlated with the cartilage and bone degradation score ($r = -0.678$, $P < 0.001$ in radiocarpal joint; $r = -0.696$, $P < 0.001$ in radiocarpal-to-MCP joint), inflammation score ($r = -0.620$, $P < 0.001$ in radiocarpal joint; $r = -0.641$, $P < 0.001$ in radiocarpal-to-MCP joint) and clinical score ($r = -0.581$, $P < 0.01$ in radiocarpal joint; $r = -0.641$, $P < 0.001$ in radiocarpal-to-MCP).

Discussion

To the best of the authors' knowledge, this is the first study to quantify both paw volume and bone volume using micro-CT in a mouse model of inflammatory arthritis. Both paw swelling and bone erosion were visible from the 3D micro-CT images in the CAIA group and corresponded to significant quantitative changes in the corresponding paw volumes and bone volumes, compared with the prednisolone-treated CAIA group. The clinical and histological assessments correlated significantly with paw swelling and bone erosion detected by micro-CT.

As expected, the micro-CT-assessed bone volume in the CAIA mice compared with the prednisolone-treated CAIA mice was significantly lower and was inversely correlated with the histological assessments, such as cartilage, bone degradation and inflammatory score, as well as the clinical paw scores [3, 29, 34, 35]. The paw volume was significantly higher in the CAIA group and directly correlated with both histological and clinical paw scores. The correlations were stronger for PV and the histological and clinical paw scores, compared with BV with these scores. This highlights the relevance of the assessment of the oedema (paw volume) as an indicator of disease severity in inflammatory arthritis models, in addition to the quantification of the bone erosion [18].

In murine models of arthritis involving micro-CT, common non-invasive methods for assessing the paw swelling are based on visual assessment or utilization of a calliper or plethysmometer [9, 10, 18]. The novel

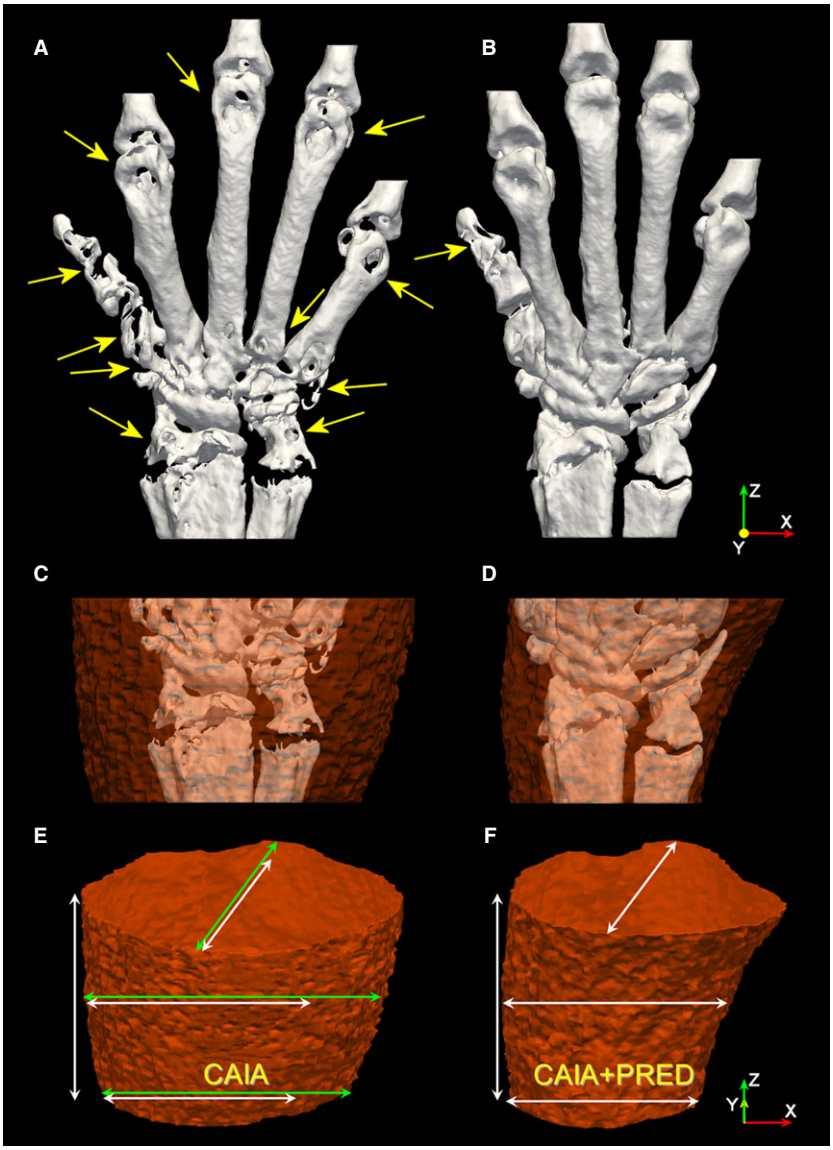

Figure 5 3D micro-CT images, front right paws. Top images (A, B): bone in white colour; the CAIA mouse (A) shows bone erosion (yellow arrows) compared with the prednisolone-treated CAIA mouse (CAIA + PRED) (B). Central and bottom images (C, D and E, F, respectively): paw volume in the radiocarpal joint in red colour [volume length 2.4 mm, vertical arrows in (E, F)]; in (C, D), the bone is visible with the soft tissue in transparency. The CAIA mouse (C, E) shows a widened paw cross section [green arrows in (E)] consistent with soft tissue swelling, compared with the prednisolone-treated CAIA mouse (CAIA+PRED) (D, F, white arrows).

micro-CT image analysis protocol developed in this study quantifies the volumetric soft tissue changes in 3D directly from the same micro-CT images used for quantifying the bone erosion. It is relatively straightforward to perform, and no additional equipment is required. Further to this, no extra preparation or treatment of the sample, such as injection of any contrast solution, is needed. The image analysis for the swelling, a post-processing procedure, can be carried out directly on the same volume of interest as used for the bone volume calculations, and can be applied on the same micro-CT scans, without the need of altering the scanning settings. In this study, the same *in vivo* system and scanning settings were used as in a live animal study previously published by our group [9]. Theoretically, this could also allow measurements of paw swelling in longitudinal study designs, where the same animals are scanned over multiple time points while under anaesthesia, as carried out for bone erosion assessments [9]. After the scan, the paw images can be realigned via software in 3D as done here, in order to have consistent positions at the different time points. Based on the results presented, this method for quantifying swelling could be included as a standard quantitative measurement tool in animal models of inflammatory arthritis where micro-CT scans are made for quantifying bone erosion.

In regard to changes in BV, the differences between groups were slightly more pronounced when analysing the radiocarpal region only (+17%), compared with the region spanning from the radiocarpal joint to the MCP joints (+14%) (Fig. 4). This is likely to be due to the location and size of the volume considered for quantification; in the larger region (radiocarpal-to-MCP joint VOI), the decrease in BV due to bone joint erosion is partially compensated by the larger quantity of bone of the carpal bones themselves,

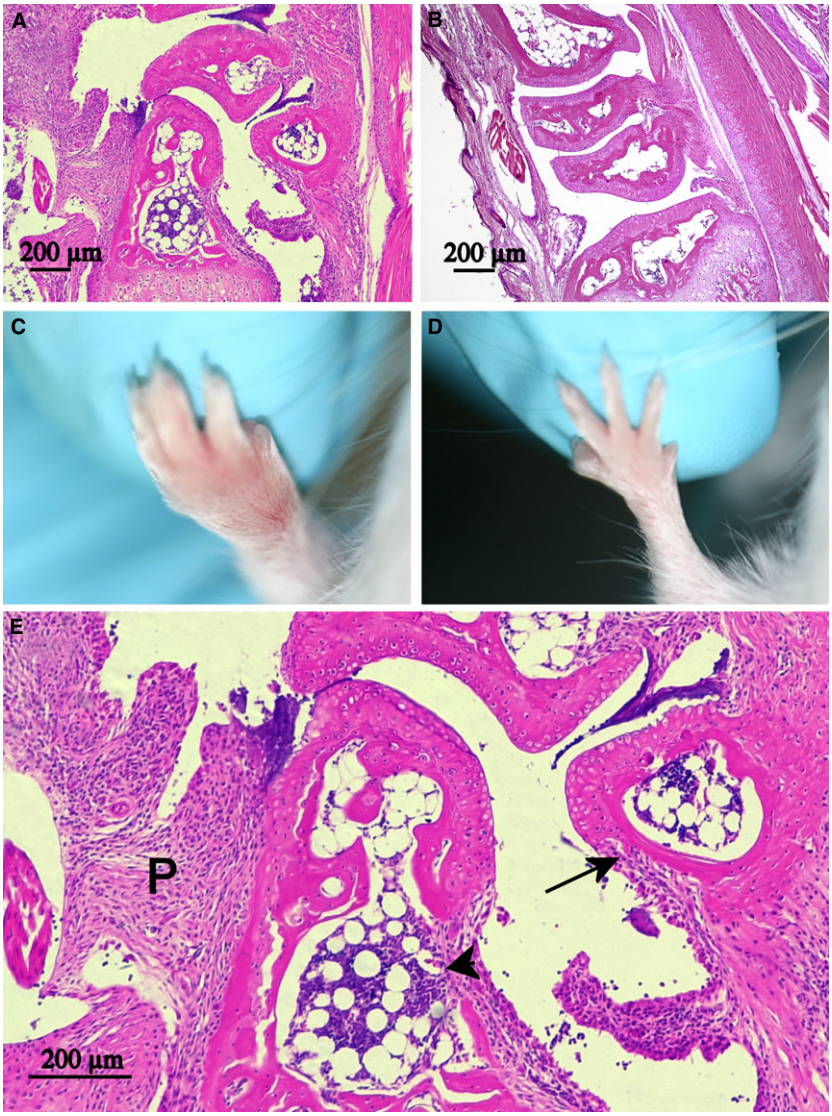

Figure 6 (A, B and E): Histologic images, haematoxylin and eosin staining. The CAIA mouse [(A) and in the corresponding close up image (E)] shows bone erosion (arrow head), cartilage degradation (arrow), pannus formation (P), compared with the prednisolone-treated CAIA mouse (B), consistent with the micro-CT images in Fig. 5A,B (bone erosion). Images in second row (C, D): Photographic images of front right paws; the CAIA mouse (C) shows paw swelling and redness, compared with the prednisolone-treated CAIA mouse (D), consistent with the widening of the paw cross section from micro-CT images in Fig. 5E versus 5F.

Table 2 Correlations (front right paws): histological and clinical scores vs. paw volume and bone volume assessed by micro-CT.

	PV_{RC}	BV_{RC}	$BV_{RC\text{-}MCP}$
Cartilage and bone degradation score	0.912***	−0.678**	−0.696**
Inflammation score	0.855***	−0.620***	−0.641**
Clinical score	0.868***	−0.581*	−0.641**

PV_{RC}, paw volume in radiocarpal joint; BV_{RC}, bone volume in radiocarpal joint; $BV_{RC\text{-}MCP}$, bone volume in radiocarpal-to-metacarpophalangeal joint.
Pearson correlation coefficient values (*r*-values).
*: $P < 0.01$; **: $P < 0.001$; ***: $P < 0.0001$.

compared with only the joints [36]. Additional attempts were also made to assess BV for the MCP joints only, which revealed changes in magnitude similar to the radiocarpal joint VOI (+17%). Hence, considering the MCP joints separately, or even the proximal interphalangeal joints as suggested by Barck *et al.* [36], may result in a further improvement in the sensitivity of the technique for measuring BV. However, for more distal joints, this is also more difficult to perform, as it requires a separate ROI for each finger; and even if the method could be automated, it still requires more attention for accurate location of the ROI in individual joints in more diseased paws [36]. Thus, based on our results regarding changes in BV, it is suggested that selecting the radiocarpal region is an appropriate, straightforward (no selection of fingers required) and sensitive method for quantification.

As a limitation of this study, we have compared the effect of CAIA in mice on PV and BV with those of a CAIA group treated with prednisolone, rather than with a normal healthy control group. Prednisolone, however, is an established RA treatment with proven efficacy, as shown also by the histological scores and clinical scores in this study and work by others [3, 29]; hence, the comparison of diseased

and treated animals is sufficient to show the validity of the presented micro-CT method. Also, we have compared and correlated the micro-CT measurements with the gold standard histological scores (scores for inflammation, cartilage and bone degradation, and pannus formation [9, 37]) and the commonly used clinical paw scores [7], but not with other methods, such as plethysmometer or calliper. In the scientific literature, the plethysmometer has been shown to be able to detect percentage changes in paw volume comparable to the present study, however mainly in rats, which have bigger paws compared with mice [10, 38, 39]. Calliper measurements for measuring changes in paw thickness (i.e. in 2D) were taken for rats and mice [3, 20, 23] and have been suggested to be preferable to plethysmometer measurements in mice [23]. However, these methods might not always be available, or even practical due to the small paws, particularly in mice. The present study on mice, supported by clinical and histological scores data, clearly shows that volumetric differences due to paw swelling can directly be quantified via a post-processing procedure, from the readily available micro-CT images for studying the bone, at micrometre resolution in 3D.

In conclusion, we present a novel and simple 3D micro-CT image analysis protocol, capable of visualizing and quantifying within the same scan not only bone erosion but also soft tissue swelling in a murine model of inflammatory arthritis. As it does not require modifications of common micro-CT scanning procedures or the use of contrast agents, and being a non-destructive imaging and quantification method, it can be easily used in antirheumatic drug studies aimed at monitoring paw swelling in 3D along with the typically assessed bone erosion using micro-CT.

Acknowledgment

The authors gratefully acknowledge Dale Caville, Discipline of Anatomy and Pathology, School of Medical Sciences, The University of Adelaide, for assistance with photography. Egon Perilli, PhD, was supported by a Grant in Aid 2013, Arthritis Australia, donor Zimmer Australia. Anak ASSK. Dharmapatni, PhD, was supported by a Grant in Aid 2012, Arthritis Australia State and Territory Affiliates, Arthritis SA.

Conflict of interest

None.

References

1 Goldring SR, Gravallese EM. Pathogenesis of bone lesions in rheumatoid arthritis. *Curr Rheumatol Rep* 2002;4:226–31.
2 Walsh NC, Crotti TN, Goldring SR, Gravallese EM. Rheumatic diseases: the effects of inflammation on bone. *Immunol Rev* 2005;208:228–51.
3 Peterson JD, Labranche TP, Vasquez KO *et al.* Optical tomographic imaging discriminates between disease-modifying anti-rheumatic drug (DMARD) and non-DMARD efficacy in collagen antibody-induced arthritis. *Arthritis Res Ther* 2010;12:R105.
4 Khachigian LM. Collagen antibody-induced arthritis. *Nat Protoc* 2006;1:2512–6.
5 Korganow AS, Ji H, Mangialaio S *et al.* From systemic T cell self-reactivity to organ-specific autoimmune disease via immunoglobulins. *Immunity* 1999;10:451–61.
6 Nandakumar KS, Andren M, Martinsson P *et al.* Induction of arthritis by single monoclonal IgG anti-collagen type II antibodies and enhancement of arthritis in mice lacking inhibitory FcgammaR-IIB. *Eur J Immunol* 2003b;33:2269–77.
7 Nandakumar KS, Svensson L, Holmdahl R. Collagen type II-specific monoclonal antibody-induced arthritis in mice: description of the disease and the influence of age, sex, and genes. *Am J Pathol* 2003;163:1827–37.
8 Terato K, Hasty KA, Reife RA, Cremer MA, Kang AH, Stuart JM. Induction of arthritis with monoclonal antibodies to collagen. *J Immunol* 1992;148:2103–8.
9 Cantley MD, Haynes DR, Marino V, Bartold PM. Pre-existing periodontitis exacerbates experimental arthritis in a mouse model. *J Clin Periodontol* 2011;38:532–41.
10 Silva MD, Savinainen A, Kapadia R *et al.* Quantitative analysis of micro-CT imaging and histopathological signatures of experimental arthritis in rats. *Mol Imaging* 2004;3:312–8.
11 Lane NE, Thompson JM, Haupt D, Kimmel DB, Modin G, Kinney JH. Acute changes in trabecular bone connectivity and osteoclast activity in the ovariectomized rat in vivo. *J Bone Miner Res* 1998;13:229–36.
12 Waarsing JH, Day JS, van der Linden JC *et al.* Detecting and tracking local changes in the tibiae of individual rats: a novel method to analyse longitudinal in vivo micro-CT data. *Bone* 2004;34:163–9.
13 Boyd SK, Davison P, Müller R, Gasser JA. Monitoring individual morphological changes over time in ovariectomized rats by in vivo micro-computed tomography. *Bone* 2006;39:854–62.
14 Perilli E, Le V, Ma B, Salmon P, Reynolds K, Fazzalari NL. Detecting early bone changes using in vivo micro-CT in ovariectomized, zoledronic acid-treated, and sham-operated rats. *Osteoporos Int* 2010;21:1371–82.
15 Botter SM, van Osch GJ, Waarsing JH *et al.* Quantification of subchondral bone changes in a murine osteoarthritis model using micro-CT. *Biorheology* 2006;43:379–88.
16 Mohan G, Perilli E, Kuliwaba JS, Humphries JM, Parkinson IH, Fazzalari NL. Application of in vivo micro-computed tomography in the temporal characterisation of subchondral bone architecture in a rat model of low-dose monosodium iodoacetate-induced osteoarthritis. *Arthritis Res Ther* 2011;13:R210.
17 Nishida S, Tsurukami H, Sakai A *et al.* Stage-dependent changes in trabecular bone turnover and osteogenic capacity of marrow cells during development of type II collagen-induced arthritis in mice. *Bone* 2002;30:872–9.
18 Chao CC, Chen SJ, Adamopoulos IE *et al.* Structural, cellular, and molecular evaluation of bone erosion in experimental models of rheumatoid arthritis: assessment by muCT, histology, and serum biomarkers. *Autoimmunity* 2010;43:642–53.
19 Chen XX, Baum W, Dwyer D *et al.* Sclerostin inhibition reverses systemic, periarticular and local bone loss in arthritis. *Ann Rheum Dis* 2013;72:1732–6.
20 Lange F, Bajtner E, Rintisch C, Nandakumar KS, Sack U, Holmdahl R. Methotrexate ameliorates T cell dependent autoimmune arthritis and encephalomyelitis but not antibody induced or fibroblast induced arthritis. *Ann Rheum Dis* 2005;64:599–605.
21 Garcia S, Bodano A, Gonzalez A, Forteza J, Gomez-Reino JJ, Conde C. Partial protection against collagen antibody-induced arthritis in PARP-1 deficient mice. *Arthritis Res Ther* 2006;8:R14.

22 Garcia S, Forteza J, Lopez-Otin C, Gomez-Reino JJ, Gonzalez A, Conde C. Matrix metalloproteinase-8 deficiency increases joint inflammation and bone erosion in the K/BxN serum-transfer arthritis model. *Arthritis Res Ther* 2010;12:R224.
23 Sharma JN, Samud AM, Asmawi MZ. Comparison between plethysmometer and micrometer methods to measure acute paw oedema for screening anti-inflammatory activity in mice. *Inflammopharmacology* 2004;12:89–94.
24 De Clerck NM, Meurrens K, Weiler H *et al.* High-resolution X-ray microtomography for the detection of lung tumors in living mice. *Neoplasia* 2004;6:374–9.
25 Haines BB, Bettano KA, Chenard M *et al.* A quantitative volumetric micro-computed tomography method to analyze lung tumors in genetically engineered mouse models. *Neoplasia* 2009;11:39–47.
26 De Langhe E, Vande Velde G, Hostens J *et al.* Quantification of lung fibrosis and emphysema in mice using automated micro-computed tomography. *PLoS ONE* 2012;7:e43123.
27 Luu YK, Lublinsky S, Ozcivici E *et al.* In vivo quantification of subcutaneous and visceral adiposity by micro-computed tomography in a small animal model. *Med Eng Phys* 2009;31:34–41.
28 Judex S, Luu YK, Ozcivici E, Adler B, Lublinsky S, Rubin CT. Quantification of adiposity in small rodents using micro-CT. *Methods* 2010;50:14–9.
29 Bender AT, Spyvee M, Satoh T *et al.* Evaluation of a candidate anti-arthritic drug using the mouse collagen antibody induced arthritis model and clinically relevant biomarkers. *Am J Transl Res* 2013;5:92–102.
30 Perilli E, Baruffaldi F, Visentin M *et al.* MicroCT examination of human bone specimens: effects of polymethylmethacrylate embedding on structural parameters. *J Microsc* 2007;225:192–200.
31 Skyscan. Description of plug-ins in custom processing, Despeckle (Sweep). *CT Analyser User Manual, Appendix A*, 2013:117. http://www.skyscan.be/next/ctan_usermanual.pdf.
32 Lorensen WE, Cline HE. Marching cubes: a high resolution 3D surface construction algorithm. *Comput Graph* 1987;21:163–9.
33 Perilli E, Briggs AM, Kantor S *et al.* Failure strength of human vertebrae: prediction using bone mineral density measured by DXA and bone volume by micro-CT. *Bone* 2012;50:1416–25.
34 Hegen M, Keith JC Jr, Collins M, Nickerson-Nutter CL. Utility of animal models for identification of potential therapeutics for rheumatoid arthritis. *Ann Rheum Dis* 2008;67:1505–15.
35 Hurtenbach U, Boggemeyer E, Stehle T, Museteanu C, Del Pozo E, Simon MM. Prednisolone reduces experimental arthritis, and inflammatory tissue destruction in SCID mice infected with Borrelia burgdorferi. *Int J Immunopharmacol* 1996;18:281–8.
36 Barck KH, Lee WP, Diehl LJ *et al.* Quantification of cortical bone loss and repair for therapeutic evaluation in collagen-induced arthritis, by micro-computed tomography and automated image analysis. *Arthritis Rheum* 2004;50:3377–86.
37 Tak PP, Smeets TJ, Daha MR *et al.* Analysis of the synovial cell infiltrate in early rheumatoid synovial tissue in relation to local disease activity. *Arthritis Rheum* 1997;40:217–25.
38 Bakhtiarian A, Aarabi Moghaddam F, Zamani MM, Ghamami SG, Farahanikia B, Khanavi M. Anti-inflammatory effect of thymus kotschyanus Boiss. & Hohen. extract on rat's hind paw edema induced by carrageenan. *J Med Plants* 2011;10:25–32.
39 Gans KR, Galbraith W, Roman RJ *et al.* Anti-inflammatory and safety profile of DuP 697, a novel orally effective prostaglandin synthesis inhibitor. *J Pharmacol Exp Ther* 1990;254:180–7.